JOURNAL OF MATERIALS SCIENCE 26 (1991) 491–496

The microstructure developments and electrical properties of calcium-modified barium titanate ceramics

TSAI-FA LIN, JIEN-LUN LIN, CHEN-TI HU
Department of Materials Science and Engineering, National Tsing Hua University, Hsinchu, 30043 Taiwan

I-NAN LIN
Chun-Shan Institute of Science and Technology, Lungtan, Taiwan

The microstructure and electrical behaviour of calcium-modified $BaTiO_3$ ceramics of compositions (a) $(Ba_{1-x}Ca_x)TiO_3$, (b) $Ba(Ti_{1-x}Ca_x)O_{3-x}$ and (c) $(Ba_{1-x/2}Ca_{x/2})(Ti_{1-x/2}Ca_{x/2})O_{3-x/2}$ have been investigated. These characteristics are observed to vary systematically with the cationic ratio, $\alpha = (Ba + Ca)/Ti$, rather than the amount (x-value) and sites that Ca^{2+} ions are supposed to occupy. A large uniform grain microstructure and normal dielectric behaviour are obtained for $\alpha \leq 1.01$ samples (groups I and II), whereas an ultra-fine grain microstructure and diffuse phase transformation (DPT) characteristics are observed for $\alpha \geq 1.08$ samples (groups III). The latter is proposed to be the suppression of tetragonal to cubic transformation due to the formation of second phase. When the sintering atmosphere is changed from air to H_2/N_2 mixture, the electrical resistivity decreases and dielectric loss increases tremendously for $\alpha = 0.99$ samples (groups I), whereas the high electrical resistivity and low dielectric loss characteristics are preserved for $\alpha \geq 1.01$ samples (groups II and III). The mechanism by which the cationic ratio improves the resistance of the materials to a reducing atmosphere is proposed to be the formation of hexagonal $BaTiO_{3-\delta}$ phase which consumes the oxygen vacancies generated.

1. Introduction

Owing to the development of integrated circuits (IC), the recent trend of electronics has been towards miniaturization of components. By this criterion, the multilayer capacitor, with good IC compatibility, excellent dielectric properties and volume efficiency surpassing all others thus becomes an indispensable component in modern electronic devices. The multilayer capacitor is produced by co-firing a laminar stack of ceramic dielectric and metal electrode layers. Because of the high sintering temperature of dielectric materials, expensive noble metals have to be used as internal electrodes in multilayer capacitors thus decreasing profitability [1–3].

In recent investigations great efforts have been made to improve the economic efficiency of multilayer capacitors [4]. One of the methods includes sintering a modified $BaTiO_3$ material in a reducing atmosphere but retaining a high electrical resistivity property such that the use of cheap nickel electrodes becomes feasible [5, 6]. The key to this modification is the promotion of the reducing atmosphere resistance of $BaTiO_3$ ceramics. Success in developing the dielectric materials for nickel-electrode multilayer capacitors has been achieved by adding acceptor-type dopant to $BaTiO_3$ ceramics [5–10].

It is reported that calcium-modified barium titanate ceramic with composition $[(Ba_{1-x}Ca_x)O]_m[(Ti_{1-y}Zr_y)O_2]$, where $0 \leq x \leq 0.20$ and $1.005 \leq m \leq 1.03$, can be co-fired with nickel electrodes in a reducing atmosphere and exhibits good dielectric performance [11]. The calcium acts as a reduction inhibitor if the value of m is slightly larger than unity. Moreover, it is generally known that Ca^{2+} ions are useful for broadening the temperature dependence of the dielectric constant (i.e. K–T curve) for $BaTiO_3$ materials [12, 13]. In other words, the CaO added to these materials is proposed to induce local compositional inhomogeneity such that the tetragonal–cubic transition of each microregion occurs at a different temperature and the resultant K–T curve is a broad one, or diffused-phase transformation (DPT) characteristics are obtained. The real mechanisms causing the DPT behaviour, and the source of the resistance to the reducing atmosphere are, however, not well understood. To resolve this ambiguity, varying amounts of calcium were added to $BaTiO_3$ in different substitutional manners in the present work. Efforts were concentrated on how the CaO influences the microstructure evolution, electrical property and the resistance to the reducing atmosphere of the $BaTiO_3$ ceramics.

0022–2461/91 $03.00 + .12

TABLE I The compositions of pure and calcium-modified $BaTiO_3$

Series	Composition formula	CaO additions	Stoichiometry modification	Code
Pure	$BaTiO_3$	None	None	P
BnT	$(Ba_{1-x}Ca_x)TiO_3$	0.08 0.15	0.01 TiO_2	B8T B15T
BnB	$(Ba_{1-x}Ca_x)TiO_3$	0.08 0.15	0.01 BaO	B8B B15B
TnT	$Ba(Ti_{1-x}Ca_x)O_{3-x}$	0.08 0.15	0.01 TiO_2	T8T T15T
TnB	$Ba(Ti_{1-x}Ca_x)O_{3-x}$	0.08 0.15	0.01 BaO	T8B T15B
PnC	$(Ba_{1-x/2}Ca_{x/2})\,(Ti_{1-x/2}Ca_{x/2})O_{3-x/2}$	0.08 0.15	None	P8C P15C

2. Experimental procedure

The samples were prepared from reagent-grade $BaCO_3$, TiO_2, and $CaCO_3$ powders (Merck Co., Darmstadt, FRG) via standard ceramic routes. As listed in Table I, the calcium oxide is added according to the formula, $(Ba_{1-x}Ca_x)TiO_3$, $Ba(Ti_{1-x}Ca_x)O_{3-x}$, and $(Ba_{1-x/2}Ca_{x/2})$ $(Ti_{1-x/2}Ca_{x/2})O_{3-x/2}$, respectively, with $x = 0.08$ or 0.15. Excess TiO_2 or BaO was added to adjust the composition stoichiometry of each series of samples and they are labelled (BnT, BnB), (TnT, TnB) and PnC, respectively.

The mixed powders were calcined at 1100 °C for 2 h in air, and the pellets made from the powders thus obtained were then sintered at 1400 °C for 2 h. The sintering atmosphere was either air or reducing atmosphere (5% H_2, 95% N_2 mixture). The bulk densities of sintered samples were determined by the Archimedes method. The microstructures of the specimens were examined, after polishing and chemical etching, using a scanning electron microscope (SEM, Joel JAX-733), and the phase constituents were identified by X-ray diffraction using a Rigaku X-ray diffractometer. Electroless-plated nickel layers were used as electrodes for electrical measurements. The temperature dependence of the dielectric properties were measured at 1 kHz, using an HP4192A impedance analyser, and the d.c. electrical resistivity at room temperature was determined from the leakage current measured with an HP4140B pA meter, under 100 V bias.

3. Results

3.1. Density and microstructure

For the pure $BaTiO_3$ sample, the grain size was larger than that of the other series samples. In the barium-site substituted samples, $(Ba_{1-x}Ca_x)TiO_3$ series, the grain size was reduced as a result of the incorporation of $CaTiO_3$, with the size being smaller for samples containing more $CaTiO_3$. Typical microstructures illustrated in Fig. 1 demonstrate that the grain size is large (≈ 35 µm) for titanium-rich samples (Fig. 1a) and is relatively small (≈ 20 µm) for barium-rich samples (Fig. 1b). The microstructure of B15T and B15B samples is similar to that of B8T and B8B samples, respectively, except that the grain size is smaller. In situations where excess CaO is added to replace either the Ti^{4+} ions only, such as $Ba(Ti_{1-x}Ca_x)O_{3-x}$ (TnT and TnB), or both the cations simultaneously, such as $(Ba_{1-x/2}Ca_{x/2})$ $(Ti_{1-x/2}Ca_{x/2})O_{3-x/2}$ (PnC), the appearance of the microstructure is quite different from that of previous samples. Two typical cases, shown in Fig. 1c and d (T8T and P8C, respectively), reveal that in addition to the ultra-fine granular structure, pores maintaining the same size as grains are distributed uniformly throughout the sample. The remarkable change in microstructure is ascribed to the presence of second phases. The pores are presumably the leftovers of etched second-phase particles, namely etching pits. Further evidence for this comes from detailed phase examinations conducted by X-ray diffraction and is discussed later. Moreover, it was observed that the T15B sample with composition $Ba(Ti_{0.85}Ca_{0.15})O_{2.85}$ + (0.01 BaO) disintegrated into a powder completely within a few hours after sintering. The existence of second phases is again suggested to be responsible for this degradation.

The sintering atmosphere, on the other hand, does not impose any significant modification on the microstructure of specimens, but it apparently influences the densification behaviour. By comparing the densities of samples sintered in a reducing atmosphere (D_{red}) with those sintered in air (D_{air}), three categories can be identified, as shown in Table II: (I) $D_{red} < D_{air}$; (II) $D_{red} \approx D_{air}$; (III) $D_{red} > D_{air}$. It is interesting to observe that the samples in group I ($D_{red} < D_{air}$), mainly BnT series samples, all possess the (Ba + Ca)/Ti ratio of 0.99, while those in group II ($D_{red} \approx D_{air}$), mainly BnB series samples, all have a (Ba + Ca)/Ti ratio of 1.01. Moreover, the samples in group III ($D_{red} > D_{air}$), including TnB, TnT and PnC series samples, correspond to samples with large (Ba + Ca)/Ti ratio ($\alpha \geq 1.08$) which even reaches a value as high as (Ba + Ca)/Ti = 1.34 for the T15T sample.

3.2. Electrical properties

The dielectric constant–temperature characteristics of sintered samples, measured in the temperature range − 25 to 150 °C are plotted in Fig. 2. The groups

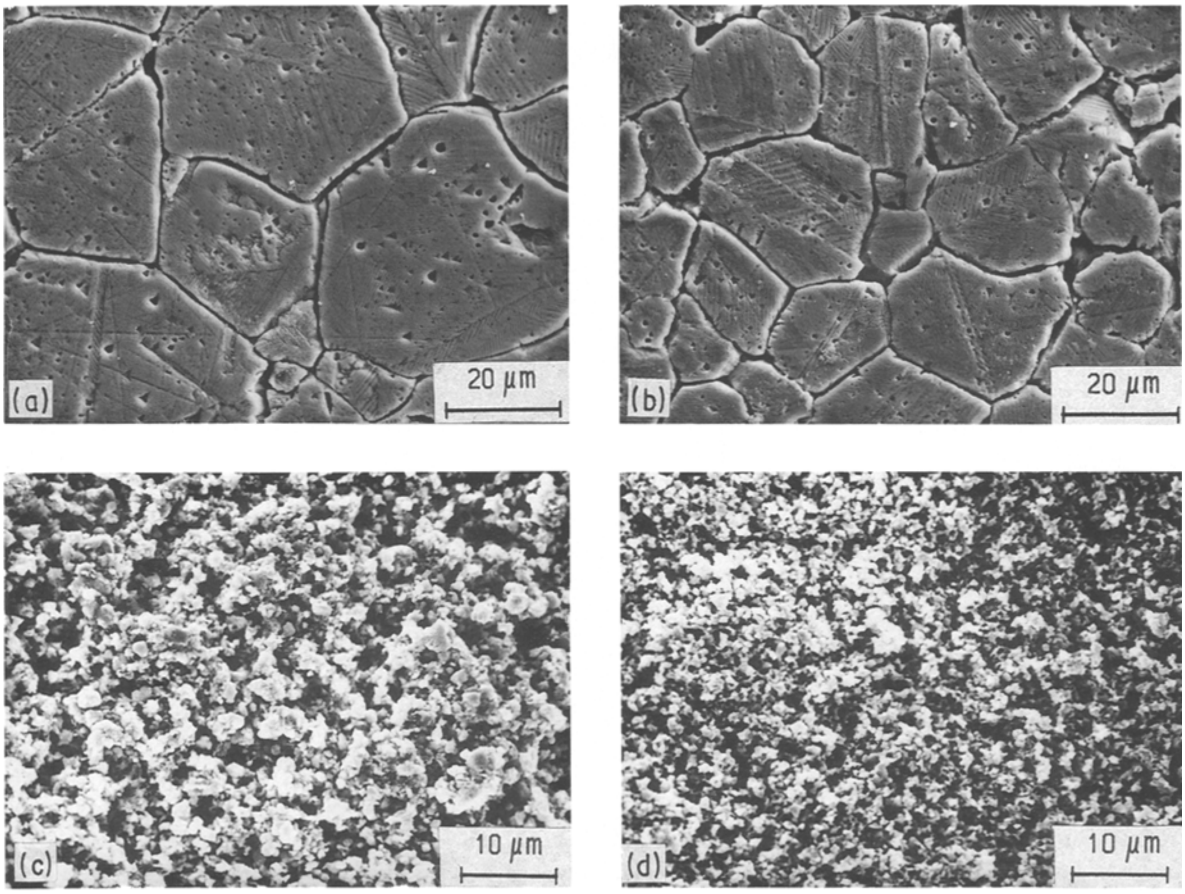

Figure 1 The effect of the addition of calcium on the microstructure of $BaTiO_3$ samples sintered at 1400 °C for 2 h in air, where the cationic ratio (Ba + Ca)/Ti, is α, (a) 0.99 for B8T, (b) 1.01 for B8B, and (c, d) $\geq$ 1.08 for T8T and P8C samples respectively.

classified in the previous section are still in use as a close relationship between the dielectric behaviour and the α-value of samples has been found. Typical K–T characteristics for pure $BaTiO_3$ samples (Fig. 2a) possesses K–T peaks corresponding to either an orthogonal–tetragonal transition (T_2) about 20 °C ($K \approx 2500$) or a tetragonal–cubic transition (T_c) about 120 °C ($K \approx 11\,000$). A large addition of CaO ($\geq 8\%$)

TABLE II The densities of samples sintered at 1400 °C for 2 h in either air (D_{air}) or reducing atmosphere (D_{red})

Sample code	D_{air} ($g\,cm^{-3}$)	D_{red} ($g\,cm^{-3}$)	Group by[a] $D_{red} - D_{air}$	(Ca + Ba)/Ti ratio
P	5.694	5.719	II	1.00
B8T	5.611	5.547	I	0.99
B15T	5.450	5.335	I	0.99
B8B	5.636	5.632	II	1.01
B15B	5.584	5.579	II	1.01
T8T	5.537	5.706	III	1.16
T15T	5.315	5.410	III	1.34
T8B	5.477	5.683	III	1.18
T15B	[b]	[b]		1.36
P8C	5.475	5.726	III	1.08
P15C	5.380	5.567	III	1.15

[a] The groups I, II, and III correspond to the samples with $D_{red} <$, $\approx$, and $> D_{air}$, respectively.

[b] T15B samples disintegrated into powder within a few hours after sintering.

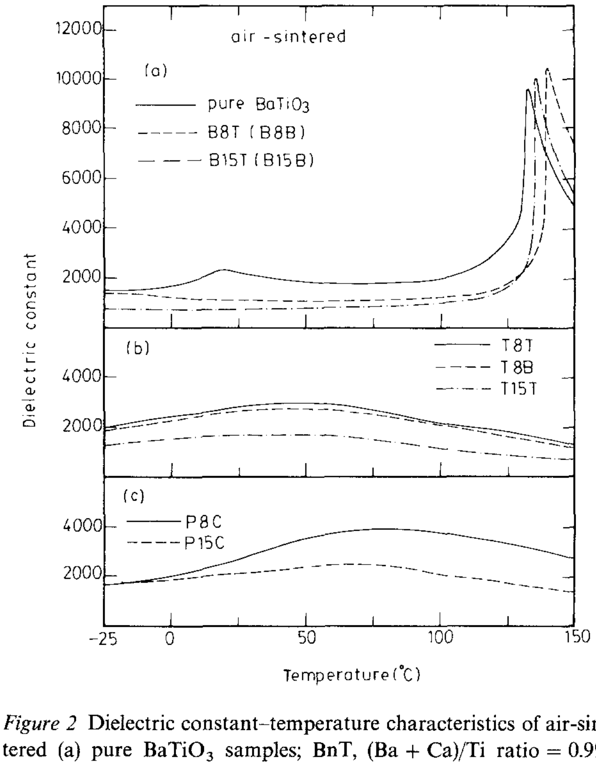

Figure 2 Dielectric constant–temperature characteristics of air-sintered (a) pure $BaTiO_3$ samples; BnT, (Ba + Ca)/Ti ratio = 0.99; BnB samples, (Ba + Ca)/Ti ratio = 1.01; (b) TnT, TnB samples; and (c) PnC samples, (Ba + Ca)/Ti ratio $\geq$ 1.08.

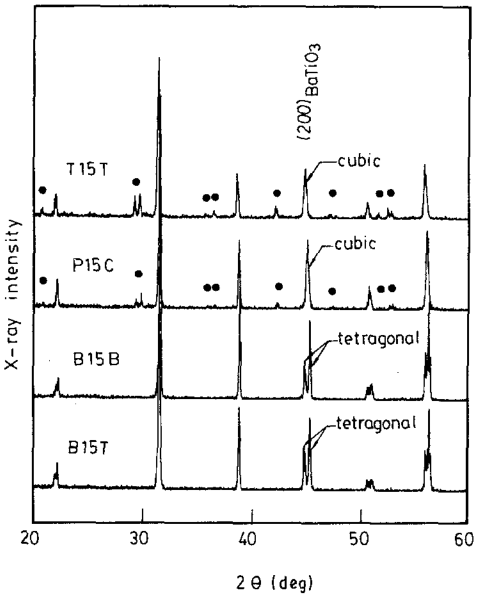

Figure 3 The X-ray diffraction pattern of the samples containing 15% CaO, i.e. B15T, B15B, P15C, and T15T samples, sintered in air. (●) $BaCaTiO_4$.

for samples in groups I and II results in a shift or suppressing of the orthorhombic–tetragonal transition peak (T_2) (Fig. 2a). However, the tetragonal–cubic transition (T_c) is still preserved and does not seem to be influenced profoundly by CaO addition. On the other hand, when a large amount ($\geq 8\%$) of CaO is added to group III samples, the K–T peaks (T_c) are suppressed appreciably and diffuse transition characteristic curves result, as shown in Fig. 2b and c (TnT, TnB, and PnC). The peak of the diffuse tetragonal–cubic transition occurred at a temperature much lower than the regular transition temperature, and the K-value decreased remarkably. The greater the CaO content, the smaller is the K-value obtained. In the limiting case, the K–T peak was completely suppressed and a flat temperature dependence of dielectric response resulted, as indicated by the K–T curve of a T15T sample in Fig. 2b. It is notable that the dielectric constant–temperature characteristics of the samples are intimately related to their microstructure. Those samples which possess sharp K–T peaks all have a relatively coarse grain structure, while those showing the diffuse dielectric response all maintain the ultra-fine grain structure. Moreover, the X-ray diffraction patterns in Fig. 3 reveal that the coarse grain samples (B15T and B15B) preserve the tetragonal perovskite structure, while the fine grain samples (T15T and P15C) consist of multiphases with the cubic perovskite structure as a major constituent.

The influence of sintering atmosphere on the K–T behaviour of sintered samples is closely related to their stoichiometry, i.e. cationic ratio $\alpha = (Ba + Ca)/Ti$. The dielectric property of group II samples ($\alpha = 1.01$) is insensitive to the variation of the sintering atmosphere (cf. Figs 4 and 2a), whereas that of samples in group I ($\alpha = 0.99$) is biased remarkably after sintering in an H_2/N_2 atmosphere (cf. Figs 4 and 2a). The dielectric constant increases appreciably with measuring temperature and an abnormally high K-value is obtained, as shown in Fig. 4. A high dielectric

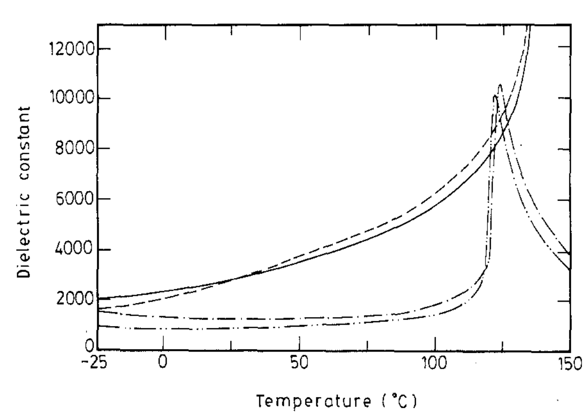

Figure 4 Dielectric constant–temperature characteristics of the H_2/N_2 sintered BnT, $\alpha = 0.99$ and BnB, $\alpha = 1.01$ samples. (——) B8T, (- - -) B15T, (—·—) B8B, (—··—) B15B.

loss factor results in associated with the high K-value samples. The microstructure corresponding to samples in groups I and II are not significantly modified when the sintering atmosphere is switched from air to H_2/N_2 mixture, that is, large grains and uniform granular structures are all preserved. The stoichiometry, i.e. the (Ba + Ca)/Ti ratio, rather than the microstructure of the samples, is considered to be the more important factor which affects the resistance to reducing atmosphere of the dielectric property. Furthermore, the sintering atmosphere results in no influence on the K–T characteristics of samples in group III. This is, again, ascribed to the high cationic ratio ($\alpha \geq 1.08$) of the samples in these groups, rather than the addition of CaO itself.

The electrical resistivity (ρ) of samples is also affected significantly by the sintering atmosphere (Fig. 5). All the samples exhibit a very high resistivity ($> 10^{10}\,\Omega$cm) after sintering in air (Fig. 5a). Most samples preserve the high resistivity property even after sintering in a reducing atmosphere, except for the

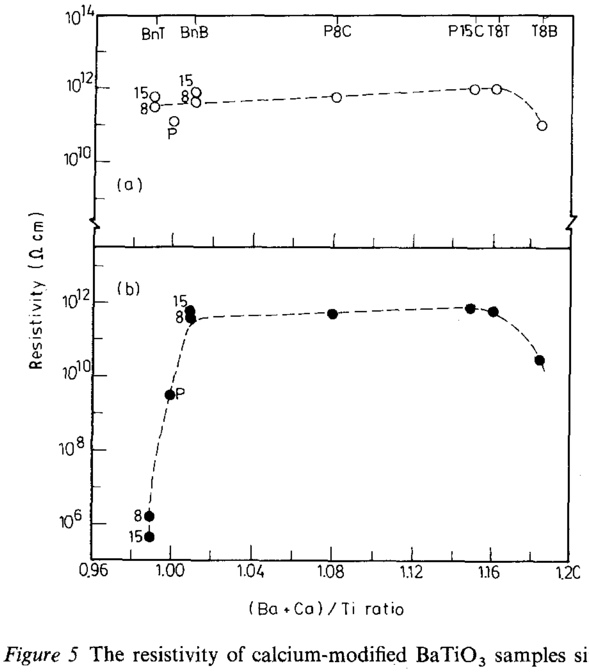

Figure 5 The resistivity of calcium-modified $BaTiO_3$ samples sintered either in (a) air (○), or (b) H_2/N_2(●), plotted against the cationic ratio, α.

TABLE III Influence of CaO addition on microstructure and electrical characteristics of $BaTiO_3$ ceramics sintered in a reducing atmosphere

Group	(Ba + Ca)/Ti ratio	Grain size	Density (D_{red} to D_{air})	*K–T* characteristics	ρ_{RT} (Ωcm)	Sample code
I	0.99	large ($\approx$ 35 μm)	$D_{red} < D_{air}$	Lossy	$\approx 10^6$	BnT
II	1.01	small ($\approx$ 20 μm)	$D_{red} \approx D_{air}$	λ-type	$> 10^{10}$	BnB
III	$\geq$ 1.08	tiny (< 1 μm)	$D_{red} > D_{air}$	DPT-type	$> 10^{10}$	TnT TnB PnC

BnT series samples where the resistivities are lowered to a value about $10^6\,\Omega$cm (Fig. 5b). It is amazing to observe that the resistivity of samples is also closely related to the (Ba + Ca)/Ti ratio. In Fig. 5b, the resistivity of samples sintered in an H_2/N_2 atmosphere is plotted against the cationic ratio, $\alpha = (Ba + Ca)/Ti$. The degradation of resistivity is observed for the sample with $\alpha < 1$, i.e. BnT samples (group I), and the high resistivities of $\alpha > 1$ samples (groups II and III) remain even after sintering in an H_2/N_2 atmosphere.

4. Discussion

The addition of CaO to $BaTiO_3$ perovskite is observed to influence the microstructure and the electrical properties of the materials profoundly, as summarized in Table III, where the samples are grouped according to the cationic ratio, α. Although in the original design, the Ca^{2+} ions are added to substitute either the Ba^{2+} ions (BnT, BnB), Ti^{4+} ions (TnT, TnB) or both of the cations (PnC), these characteristics, however, do not vary according to at which sites the Ca^{2+} ions are supposed to replace the other cations. On the contrary, they vary systematically with the (Ba + Ca)/Ti ratio (α).

Precipitation of second phase when the Ca^{2+} ions are added to replace either the Ti^{4+} ions (Tn series) or both of the cations simultaneously (Pn series). This phenomenon infers that solid solution of CaO with $BaTiO_3$ materials can only happen for Bn series samples where the Ca^{2+} ions are added to substitute the Ba^{2+} ions. In other words, the incorporation of Ca^{2+} ions occurs preferentially at the Ba^{2+} sites rather than the Ti^{4+} sites. The samples in group III (Tn and Pn series) will then contain many more Ba^{2+} site ions than Ti^{4+} site ions ($\alpha \geq 1.08$). Larger amounts of second phases are then expected which in turn results in tiny grain microstructure. This is in accord with the microstructure and X-ray diffraction results (Figs 1 and 3).

It has been proposed that in $BaTiO_3$ capacitor materials, the $CaTiO_3$ incorporated will result in the depression of *K–T* peaks without shifting the Curie temperature (T_c) [12, 13]. The mechanisms by which the CaO modifies the dielectric behaviour is, however, not well understood. A possible explanation is that the CaO added induces a localized compositional inhomogeneity such that there exist microregions of different T_c-value [13]. The diffused-phase transformation (DPT) characteristics are the result of the *K–T* behaviour of these microregions. The observation that the microstructures and dielectric properties of BnB and BnT samples are not modified significantly (Figs 1 and 2), even when 15 mol % Ba^{2+} ions are replaced by Ca^{2+} ions, indicates that the solubility of CaO in $BaTiO_3$ materials is quite high as long as the Ca^{2+} ions are added to substitute the Ba^{2+} ions, or following the formula $(Ba_{1-x}Ca_x)TiO_3$. Moreover, the DPT characteristics are observed only in Tn and Pn series samples. The formation of a microregion is therefore not a plausible mechanism for the occurrence of DPT dielectric behaviour in this material. It is believed, on the contrary, that the suppression of cubic–tetragonal phase transformation due to the refinement of the granular structure, as observed in the group III (Tn and Pn series) samples, is the genuine mechanism which results in the DPT characteristics. This is in accord with the observations of Hagemann *et al.* [1].

Concerning the mechanisms by which the CaO addition improves the resistance to reducing atmosphere of the $BaTiO_3$ ceramics, detailed examination of the results in Fig. 5 reveals that the cationic ratio (α) is the more probable cause, rather than the amount of CaO included. This is evident by the fact that addition of even up to 15 mol % CaO in B15T samples does not result in high resistivity, while the same amount of CaO addition in B15B samples can preserve the high ρ-value, when they are sintered in an H_2/N_2 atmosphere. The subtle difference in the two series of samples is the value of the cationic ratio (A = Ba + Ca/Ti), i.e. $\alpha = 0.99$ for BnT and $\alpha = 1.01$ for BnB samples. In addition, all the samples which are resistant to a reducing atmosphere, such as Tn and Pn series, have the cationic ratio $\alpha \geq 1.08$, as indicated in Table III.

Because the formation of oxygen vacancies (V_O) is inevitable when the $BaTiO_3$ materials are exposed to a reducing atmosphere, the V_O will act as electronic donors [14]. The preservation of high resistivity for $\alpha \geq 1.01$ samples, when sintered in an H_2/N_2 atmosphere, must be due to the suppression of either the charge carriers or the electronic donors. The former mechanism will need electronic traps and has been proposed to be the formation of acceptor states resulting from the substitution of Ti^{4+} ions by Ca^{2+} ions, i.e. Ca''_{Ti} acceptors [5, 15, 16]. This is, however, not in accord with our observations, because both the microstructure and dielectric characteristics favour the model where Ca^{2+} ions occupy the Ba^{2+} sites. The suppression of electronic donors, oxygen vacancies, is thus the only possible mechanism which can make the materials resistant to the H_2/N_2 atmosphere. But how can this be? The formation of hexagonal phase of the composition $BaTiO_{3-\delta}$ is thought to be the possible mechanism. According to previous research [17, 18], on the phase equilibrium of the $BaTiO_3$ system, it is known that the transformation of perovskite to hexagonal structure is enhanced when the Ba/Ti ratio is slightly larger than one and in the presence of oxygen vacancies, because the hexagonal structure possesses face-sharing octahedra, while the tetragonal structure has corner-sharing ones. In other words, the formation of hexagonal phases will consume the V_O such that the source of electronic donors is reduced significantly and the resistivity of $\alpha > 1$ samples is not lowered even when sintered in a reducing atmosphere. It is, therefore, concluded that the cationic ratio, α, is the only important factor, and whether the Ba^{2+} sites consist of Ba^{2+} ions only, or of a $(Ba^{2+} + Ca^{2+})$ ion mixture, does not matter, in order to increase the resistance to reducing atmosphere of the $BaTiO_3$ materials.

5. Conclusions

1. The microstructure evolution and electrical response of calcium-modified barium titanate ceramics reveal that the Ca^{2+} ions probably occupy barium sites of $BaTiO_3$ perovskite, rather than replacing the titanium sites, as indicated by the following observations:

(i) large grain structure and normal K–T behaviour for $(Ba_{1-x}Ca_x)TiO_3$ materials.
(ii) ultra-fine grain structure accompanied by second-phase precipitation and a diffuse-phase transformation (DPT) characteristic for $Ba(Ti_{1-x}Ca_x)O_{3-x}$ and $(Ba_{1-x/2}Ca_{x/2})(Ti_{1-x/2}Ca_{x/2})O_{3-x/2}$ materials.

2. The DPT characteristics of the samples with (Ba + Ca)/Ti $\geq$ 1.08 is possibly due to the suppression of the tetragonal–cubic transformation which, in turn, is the result of ultra-fine grain microstructure induced by the inhibition of grain growth in the presence of second phases.

3. The formation of hexagonal phase induced by a high cationic ratio, (Ba + Ca)/Ti $\geq$ 1.01, of the material in the presence of oxygen vacancies is proposed to be the mechanism which makes the materials resistant to a reducing atmosphere.

References

1. H. -J. HAGEMANN, D. HENNINGS and R. WERNICKE, *Philips Tech. Rev.* **41** (1983/84) 89.
2. D. HENNINGS, *Int. J. High Tech. Ceram.* **3** (1987) 91.
3. W. R. BUESSEM and T. I. PROKOPOWICZ, *Ferroelectrics* **10** (1976) 255.
4. J. M. HERBERT, in "Ceramic Dielectrics and Capacitors" (Gordon and Breach, New York, London, Paris, Montreux, Tokyo, 1985) Ch. 6.
5. Y. SAKABE, *Amer. Ceram. Soc. Bull.* **66** (1987) 1338.
6. I. BURN, *ibid.* **57** (1978) 600.
7. I. BURN and G. H. MAHER, *J. Mater. Sci.* **10** (1975) 633.
8. I. BURN, *ibid.* **14** (1979) 2453.
9. H. -J. HAGEMANN and H. IHRIG, *Z. Phys. B. Condens. Matter* **20** (1979) 3871.
10. H. -J. HAGEMANN and D. HENNINGS, *J. Amer. Ceram. Soc.* **64** (1981) 590.
11. Y. SAKABE and H. SENO, U.S. Pat. 4115493 (1978).
12. G. H. JONKER, *Philips Tech. Rev.* **17** (1955/56) 129.
13. V. F. CAPOZZI, in "Multilayer Ceramic Capacitor Materials and Manufacture" (Oxy Metal Industries Co. New York, 1975) p. 33.
14. J. DANIELS and K. H. HÄRDTL, *Philips Res. Rept* **31** (1976) 489.
15. Y. H. HAN, J. B. APPLEBY and D. M. SMYTH, *J. Amer. Ceram. Soc.* **70** (1987) 96.
16. X. W. ZHANG, Y. H. HAN, M. LAL and D. M. SMYTH, *ibid.* **70** (1987) 100.
17. D. E. ROSE and R. ROY, *ibid.* **38** (1955) 102.
18. H. AREND and L. KIHLBORG, *ibid.* **52** (1969) 63.

Received 25 July 1989
and accepted 19 February 1990